Energy Conversion and Management 114 (2016) 290–302

Contents lists available at ScienceDirect

Energy Conversion and Management

journal homepage: www.elsevier.com/locate/enconman

Numerical and experimental investigation on effects of inlet humidity and fuel flow rate and oxidant on the performance on polymer fuel cell

Pourya Karimi Takalloo, Ehsan Shabahang Nia, Mohsen Ghazikhani *

Department of Mechanical Engineering, School of Engineering, Ferdowsi University of Mashhad, P.O. Box No. 91775-1111, Mashhad, Iran

ARTICLE INFO

Article history:
Received 19 July 2015
Accepted 30 January 2016

Keywords:
Polymer fuel cell
Electro-chemical process
Cell performance
Polarity curve
Simulation

ABSTRACT

Considering the importance of water management in a fuel cell and in order to increase the rate of the electro-chemical process in fuel cells with polymer membrane, it is required to optimize the humidity and inlet flow rates on anode and cathode sides. In this study, the impact of alteration in humidification and inlet flow rates on performance improvements for polymer membrane fuel cells is investigated both experimentally and numerically. To obtain the objective, employing the results from experiments and simulations, polarity curve and power density are produced and further used to conduct the desired investigations. In addition, through the conducted simulations the effects of using pure oxygen in the cathode side and inlet gas temperatures on the polarity curve is studied. The results demonstrate that an increase in humidity of the inlet gases will lead to performance amelioration in the cell, due to reduction in ionic resistance at the membrane. Furthermore, with the aforementioned increment; molar fractions of hydrogen and oxygen are decreased through the channel which results in produced water increment. Amplification in inlet flow rates to a certain level will improve the penetration possibility for gaseous forms leading to betterment of the cell performance in this specified range. Performance improvements with inlet gases temperature increment conclude other results of this study.

1. Introduction

Developing novel and efficient methods for fuel energy transformation to usable end energy, is considered a serious challenge in the contemporary world. Fuel cell technology has been developed as a direct fuel chemical energy conversion process which utilizes an electro-chemical phenomenon [1]. Polymer fuel cell possesses advantages such as high efficiency, solid electrolyte, electrical energy production without pollution, variety, noiseless performance, and considerably short start up time. The major challenge in a polymer membrane fuel cell includes water and heat management which is deemed influential in optimal performance of the fuel cell. When the membrane is humidified on a desired level, strong ionic conduction occurs in electrolytes leading to efficiency ameliorations. Note that in case with excess water in comparison with the optimal condition, the porous region for gas penetration will be flooded which will impose limitations on gas transfer to reaction layer and the voltage of the cell experience drop. In order to obtain high performance rates in a fuel cell, the water amount in the membrane should be optimized, this is achieved via humidification of reactor gases before they enter the cell or regulations in humidity levels. Inlet flow rate and oxidant control can be considered as other influential parameters. In addition, since high temperature in the cell will cause ionic conduction deterioration due to drying in membrane and low temperatures will decrease the reaction rates and cause internal losses, temperature management in the cell stands out as a key parameter [2,3]. In the recent decades several studies targeted fuel cells performance in different conditions. Iranzo et al. [4] experimentally investigated the effects of parameters such as relative humidity of the inlet gasses on anode and cathode sides and air stoichiometry on the cathode side on the performance of fuel cell with spiral channels. The results showed that anode humidification has been more effective in comparison with cathode humidification. In order to improve the performance this humidification is very effective and leads to decrease in ionic resistance and performance enhancement. This phenomenon occurs in low current densities while in high current densities the cathode size requires less humidification due to more water production. Mulyazmi et al. [5] investigated the water balance in a PEM fuel cell by using the water transfer phenomenon. Their results indicated that the water diffusion from the cathode to the anode was not observed when the relative values of humidity were 20% and 58% for the cathode and anode, respectively. In addition, they observed a minimum concentration

* Corresponding author. Tel.: +98 511 8673304x209; fax: +98 511 8673304.
E-mail address: ghazikhani@ferdowsi.um.ac.ir (M. Ghazikhani).

http://dx.doi.org/10.1016/j.enconman.2016.01.075
0196-8904/

value of condensed water at gas inlet humidity and temperatures between 45–89% and 343–363 K, respectively.

Al-Zeyoudi et al. [6] evaluated the performance of an open-cathode polymer electrolyte membrane fuel cell. This research indicated that the performance is improved considerable by the anode humidification under arid and hot weather. Bozorgnezhad et al. [7] performed an experimental study on the two-phase flow in the cathode channel of a PEMFC (proton exchange membrane fuel cell). Their results showed that controlling the amount of flow rate of the oxygen and fuel (that concerns to the Stoichiometry of inlet gases directly) is one of the important and effective parameters on the operating of fuel cell.

Reshetenko et al. [8] investigated the effects of gas humidification on performance of PEMFC. Several parameters such as Ohmic, concentration and activation losses are analyzed to determine the performance of fuel cell. They found that the Ohmic and activation losses increase with decrease in a relative humidity. Sreenivasulu et al. [9,10] evaluated performance parameters in a fuel cell with proton exchange membrane consisting of four spiral channels both experimentally and through simulations. The results demonstrated that in low and medium current densities increment in relative humidity within 10–65% results in performance improvement while in high current density the vice versa trend is observed due to water accumulation in cathode size, the results also revealed that with increase in fuel and oxidant flow rates and the performance will experience betterment.

Wang et al. [11] investigated about the role of the humidity of anode and cathode inlet on the improvement of electrical operation of the fuel cell using two dimensional and two phase model and the results showed that the maximum power density of a fuel cell is dependent on the qualification of the humidity of anode and cathode sides. The effect of the different amounts of relative humidity and Stoichiometry of the air on the operation of fuel cell has been checked by the polarity curve and it shows that the increasing of humidity improves the operation of fuel cell.

Yuan et al. [12], evaluated the impact of various parameters on the performance of a fuel cell through a 3D multi-phase model, parameters such as relative humidity of the reactor gasses and air stoichiometry were included. The results showed that humidification on anode side will be more efficient since there is water produced on the cathode side while the anode side experiences drying, in addition; elevation in air stoichiometry rate, will improve the rate of water guidance toward the exit of the channel, and increase the amount of oxygen and consequently will ameliorate the rate of chemical reactions which will lead to cell performance betterment. Dong et al. [13] studied the effect of cathode relative humidity on polymer fuel cell for vehicle application, in these investigations low relative humidity led to low voltages in the fuel cell and also ununiformed distributions of current density and temperature were observed. Rosli et al. [14] after investigations on a transparent spiral single cell polymer membrane revealed that a spiral channel will pass the accumulated water quite easily and in the case of dry cathode there is no liquid water detectable on the anode side; the dried membrane and cell power decrease due to increment in ionic resistance. Afshari et al. [15] analyzed a type of polymer membrane fuel cell for application in vehicles the results of which demonstrated that in high outlet voltages where no phase change occur, increment in humidity percentage and reduction in inlet flow rate will have a positive impact on cell performance; however, in low outlet voltages, the performance of fuel cell experiences deterioration with increase in humidity percentage and reduction in inlet flow rate. It was also showed that increase in pressure and temperature will lead to performance amelioration in a wide range for outlet voltages.

In most researches, air has been assumed instead of the inlet flow of the cathode side. In this case the electrochemical reaction of fuel cell happens poorly because of decreasing contact area of cathode pole than the case with pure oxygen. In this investigation we have used pure oxygen in a role of oxidant in the cathode side to improve efficiency of fuel cell and it does better as we expected. Also for preventing the problems because of water flooding in channels we have used 4-Serpentin flow channel with elliptical cross section geometry and for achieving exact and trusted numerical results, we have compared all of the experimental results with numerical results that they have good agreements.

2. Fuel cell test set up

Through utilizing the experimental set up, various parameters including pressure and inlet flow rate of hydrogen and oxygen, humidity and temperature of inlet gases, temperature of the fuel cell body and also current and voltage of fuel cell are measurable. Fig. 1 depicts the polymer fuel cell set up and its respective circuit.

The characteristics of the aforementioned experimental set up are presented as follow:

- The set up possesses the capability of monitoring and controlling of inlet fuel flows and oxidant to fuel cell.
- The set-up is capable of monitoring and controlling inlet and outlet flow rates of oxygen and hydrogen.
- The set up includes a humidification system for oxygen and hydrogen gases.
- The set up possesses the capability of monitoring and controlling inlet and outlet gases temperature.
- The set up possesses the capability of monitoring and controlling fuel cell body temperature.
- The electrical charge of the set up is resistive.
- The set up possesses the capability of monitoring and controlling inlet and outlet gases pressure.
- The set up is capable of alarming about hydrogen leakage in the environment.

The range of polymer fuel cell test set up performance and also the conditions required for the conducted experiments is presented in Table 1.

Through the conducted experiments a single cell fuel cell weighted 1300 g is employed, dimensions of the system include $101 * 95 * 45\ mm^3$ and the active surface is equal to $25\ cm^2$ as delineated in Fig. 2, the vertical section of channels for fuel and oxidant is elliptic, dimensions of this section include $1 * 1.27\ mm^2$.

Channels for fuel flow and oxidant which is furrowed on bi-polar planes is formed in a four way spiral manner, geometrical characteristics are presented in Table 2.

3. Fuel cell model characteristics

As it is depicted in Fig. 3, the proposed model for fuel cell includes all parts for flow channels, gas penetration, catalyst, and proton exchange membrane layers. In this model hydrogen is utilized as fuel on the anode side while oxygen is deployed as oxidant on the cathode side. In the present model the inlet gases flow is parallel in the channels, it is assumed that the mixture of the gases is ideal and due to low velocities and consumption rates, the flow is considered incompressible and laminar. The amount of porosity in various regions, is considered to be constant due to homogenous nature assumption for this region, the model is deemed to be dominated by the steady state nature and the processes is analogous for all the channels.

A section of the utilized grid for numerical simulation is shown in Fig. 4, the number of nodes after mesh independency studies is equal to 594,720. In catalyst, membrane, flow channels, and gas

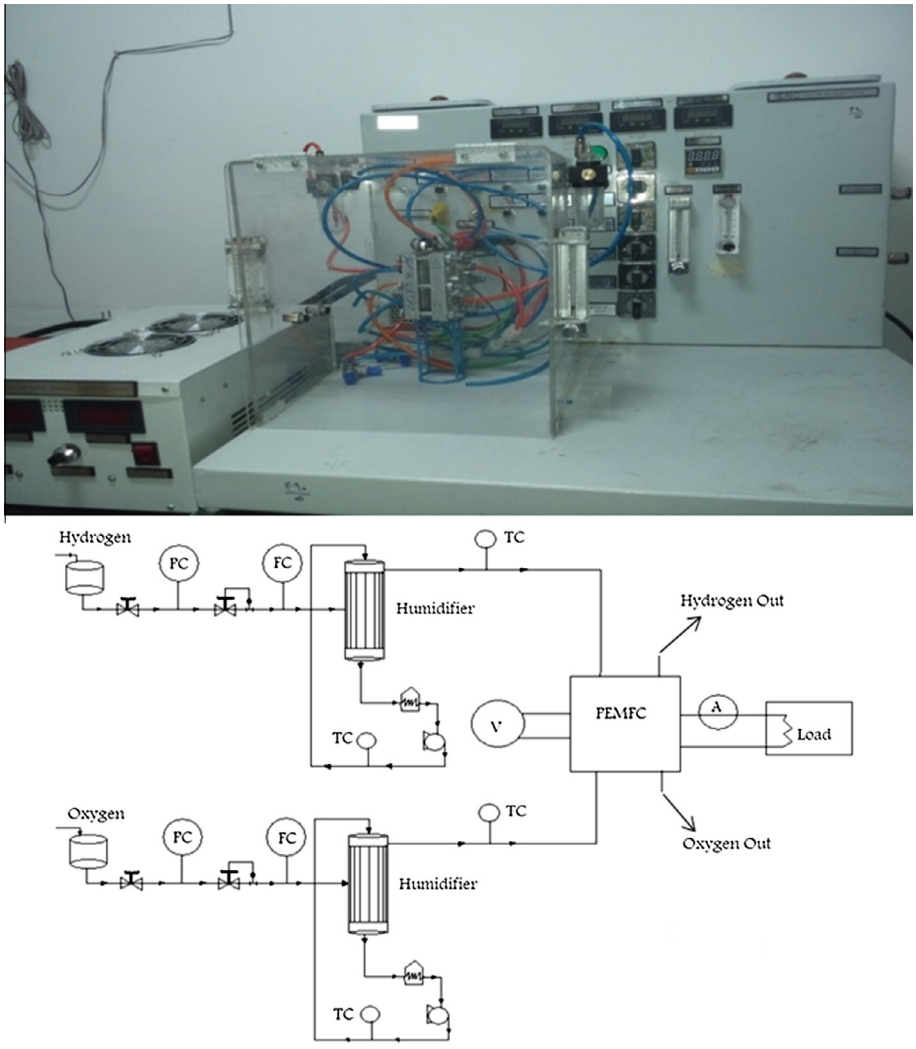

Fig. 1. Polymer membrane fuel cell test set up and its performance circuit.

Table 1
The range of polymer fuel cell test set up performance and the conditions required for the conducted experiments.

Operational characteristic of the test bench		Range of changing the parameters in this study	
Voltage	0–2 V	Oxygen flow rate	0.5 l min^{-1}
Current	0–20 A	Hydrogen flow rate	0.3 l min^{-1}
Power	0–22 W	Oxygen/hydrogen temperature	45–65 °C
Flow rate	0–2 l min^{-1}	Anode/cathode inlet pressure	3 bar
Gas & cell temperature	40–80 °C		

penetration layers parts, the regions close to catalyst region include finer meshing strategy.

3.1. Governing equations

Generally the governing equations for physical processes in a polymer fuel cell consists of mass, momentum, energy, chemical forms, and electrical charge conservation which are presented as follows

$$\frac{\partial(\varepsilon\rho)}{\partial t} + \nabla\cdot(\varepsilon\rho\vec{u}) = 0 \quad (1)$$

$$\frac{\partial(\varepsilon\rho\vec{u})}{\partial t} + \nabla\cdot(\varepsilon\rho\vec{u}\vec{u}) = -\varepsilon\nabla P + \nabla\cdot(\varepsilon\mu^{\text{eff}}\nabla\vec{u}) + S_u \quad (2)$$

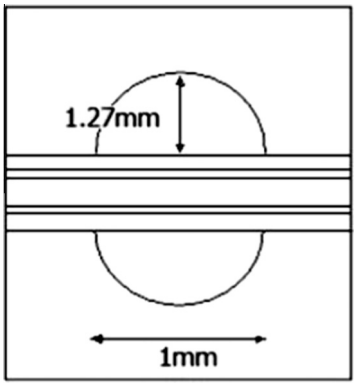

Fig. 2. Cross section of the flow/current channel.

Table 2
Geometrical characteristics of the model fuel cell.

Region	Size (mm)
Bi-polar planes thickness	5
Gas penetration layer thickness	0.33
Catalyst layer thickness	0.01
Membrane thickness	0.051
Length of each channel	48
Width of the channel	1
Depth of the channel	1.27
Distance between channels	0.8

$$(\rho c_p)_{\text{eff}}\frac{\partial T}{\partial t}+(\rho c_p)_{\text{eff}}(\vec{u}\cdot\nabla T)=\nabla\cdot(k_{\text{eff}}\nabla T)+S_e \tag{3}$$

$$\frac{\partial(\varepsilon X_k)}{\partial t}+\nabla\cdot(\varepsilon\vec{u}X_k)=\nabla\cdot(D_k^{\text{eff}}\nabla X_k)+S_k \tag{4}$$

$$\nabla(\sigma_e^{\text{eff}}\nabla\varphi_e)+S_{\varphi_e}=0 \tag{5}$$

where u, P, T, ρ, μ, ε, k_{eff}, c_p, X_k, φ_e represent velocity vector, pressure, temperature, fluid density, mixture mean viscosity, porosity coefficient, thermal conduction, mixture mean specific heat coefficient, molar fraction of the ingredient k, and electrical potential in electrolyte and electrode respectively.

The effective dissemination coefficient of the ingredient k and membrane ionic conduction coefficient are obtained via following equations [16].

$$D_k^{\text{eff}}=\varepsilon^{1.5}D_k \tag{6}$$

$$\sigma_k^{\text{eff}}=\varepsilon^{1.5}\sigma_k \tag{7}$$

Dissemination coefficient is dependent to temperature and pressure through the following equation.

$$D(T)=D_0\left(\frac{T}{T_0}\right)^{\frac{3}{2}}\left(\frac{P_0}{P}\right) \tag{8}$$

Protonic conduction coefficient in membrane phase is also a function of temperature and the amount of water in the membrane [17]

$$\sigma_m(T)=100\exp\left[1268\left(\frac{1}{303}-\frac{1}{T}\right)\right]\times(0.005139\lambda-0.00326) \tag{9}$$

According to the following equations, the water in the membrane, λ, depends on the water activity parameter, a [18]

$$\lambda=\begin{cases}0.043+17.18a-39.85a^2+36a^3 & 0<a\le 1\\ 14+1.4(a-1) & 1\le a\le 3\end{cases} \tag{10}$$

$$a=\frac{X_{H_2O}P}{P^{\text{sat}}} \tag{11}$$

Water dissemination coefficient in the membrane is obtained as follows

$$D_w^m=\begin{cases}3.1\times10^7\times\lambda(e^{0.28\lambda}-1)e^{(\frac{2346}{T})} & 0<\lambda<3\\ 4.17\times10^8\times\lambda(161e^{\lambda}+1)e^{(\frac{2346}{T})} & 3<\lambda\end{cases} \tag{12}$$

Hydrogen, oxygen and water dissemination coefficients in the gas mixture is a function of temperature and pressure

$$D_{H_2}=1.1\times10^4\left(\frac{T}{353}\right)^{3/2}\left(\frac{1}{P}\right) \tag{13}$$

$$D_{O_2}=3.2\times10^5\left(\frac{T}{353}\right)^{3/2}\left(\frac{1}{P}\right) \tag{14}$$

$$D_{H_2O}=7.35\times10^5\left(\frac{T}{353}\right)^{3/2}\left(\frac{1}{P}\right) \tag{15}$$

The density of the axial current is calculated as follows

$$I(y)=-\sigma_e^{\text{eff}}\frac{\partial\varphi_e}{\partial x}|_{x=IF} \tag{16}$$

$$I_{\text{avg}}=\frac{1}{L}\int_0^L I(y)dy \tag{17}$$

And the density of the current is evaluated using the following equations [19]

$$j_a=aj_{0,a}^{\text{ref}}\left(\frac{X_{H_2}}{X_{H_2,\text{ref}}}\right)^{\frac{1}{2}}\left(\frac{\alpha_a+\alpha_c}{RT}\cdot F\cdot\eta\right) \tag{18}$$

$$j_c=aj_{0,c}^{\text{ref}}\left(\frac{X_{O_2}}{X_{O_2,\text{ref}}}\right)^{\frac{1}{2}}\exp\left(\frac{-\alpha_c}{RT}\cdot F\cdot\eta\right) \tag{19}$$

$$\eta(x,y)=\varphi_s-\varphi_e-V_{oc} \tag{20}$$

In the above equations j, α, η and V_{oc} stand for transferred current density, transfer coefficient, excess voltage, and open circuit voltage respectively.

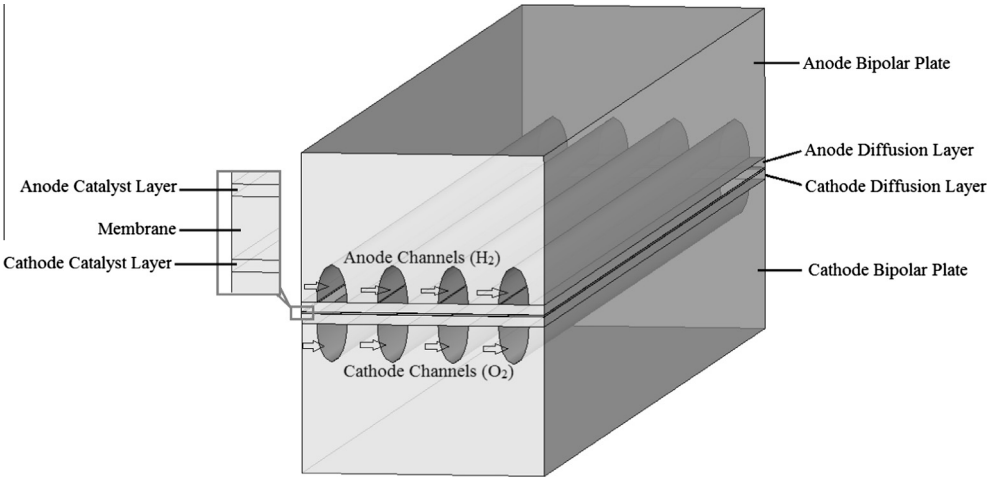

Fig. 3. Structure of a polymer membrane fuel cell.

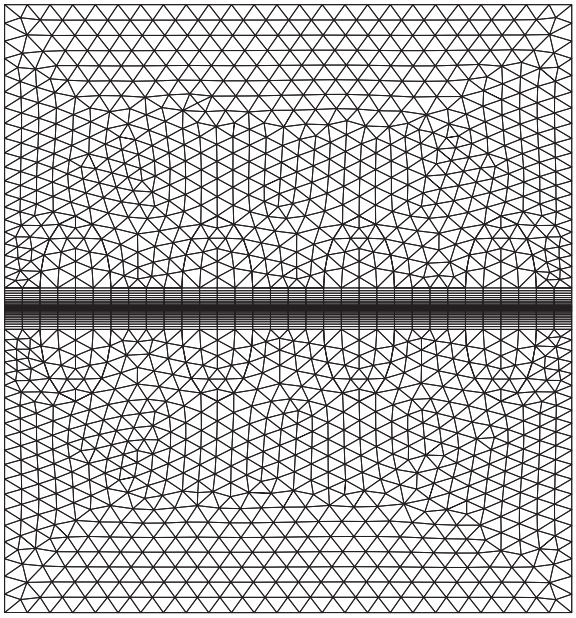

Fig. 4. Close view of the grid for fuel cell model.

Table 3 includes the respective source terms for the above equations on different regions of the cell.

3.1.1. Numerical method and boundary conditions

The considered 3D model is single phase and steady state which includes continuity equations in different parts of the cell. With employing this model on can calculate fuel cell's parameters in various nodes.

To solving mass conversion, momentum, chemical Species and electrical charge equations, we need boundary conditions of different areas of fuel cell, but many of them are not clear. Subsequently the obtained results from equations aren't exact. Also every area has its own equations and these equations are connected with boundary conditions to together and the problem becomes complicated. We don't need internal boundary conditions between various layers of fuel cell in the single zone method and the external boundary conditions are adequate. Not applying these boundary conditions, increases the accuracy of results and facilitates solving of equations, however the time of solving of equations will be so long. It is possible one equation does not work in a specific zone by applying single zone method but in numerical approach, with applying the source term big mountain and determining physical features related to that area, it is possible to develop and use the equation similarly in all areas and not using different equations in each zone.

Generally, conditions for channels inlet and outlet regions, and also anode and cathode terminals need to be determined. In flow inlet for channels on anode and cathode sides, pressure, temperature, mass flow rate, and molar fraction should be known, and the boundary conditions for velocities and outlet ingredients are considered fully developed. Electrical potential is deemed to be zero on the anode side, and equal to $\phi = V_{cell}$ for the shared face between the catalyst and the gas penetration layers. Actually, for external boundaries which are the passage for electrons, the amount of voltage is considered equal to zero on the anode side while it is deemed equal to cell voltage on the cathode side. The zero flux boundary condition is employed for all the external boundaries with exceptions for inlet and outlet boundaries.

Finite volume approach with a "Simple" algorithm is deployed to solve the governing equations. The performance conditions for the cell and parameters utilized in the simulation system are presented in Table 4. The commercial software "Ansys Fluent" is used in order to apply the discussed the numerical method.

Fluent software uses Multigrid method in the pressure based solver. This method improves the speed of solution convergency by correcting the calculations on the coarse grid levels. In the Multigrid methods calculation must pass over from fine grid level to big one and inversely. There are so many methods in the manner and Sequence of these transitions that we know them in the title of Multigrid cycles. In this model we have used *F*-cycle.

4. Results and discussion

4.1. Validating numerical simulation

In order to ensure the numerical approach validity, the polarity curve obtained from it are compared against the one achieved through experimental method. Fig. 5 provides comparison between polarity curves obtained from numerical and experimental approaches in a condition with temperature equal to 55 °C and a pressure of 3 bars, mass flow rate on the anode and cathode sides are 0.3 and 0.5 l/min respectively, and the humidity percentage for

Table 4
Performance conditions and utilized parameters.

Parameters	Value
Faraday constant	96,487 C mol^{-1}
Oxygen flow rate	0.5 l min^{-1}
Hydrogen flow rate	0.3 l min^{-1}
Inlet gases temperature	328 K
Inlet gases pressure	3 bar
Anode ref. current density	1e8
Cathode ref. current density	650
Anode concentration exponent	0.5
Cathode concentration exponent	1
Reference diffusivity of H_2	11e−5 m^2 s^{-1}
Reference diffusivity of O_2	3.2e−5 m^2 s^{-1}
Reference diffusivity of H_2O	7.35e−5 m^2 s^{-1}
Reference diffusivity of other species	1.1e−5 m^2 s^{-1}
Porosity of gas diffusion layer	0.5
Porosity of gas catalyst layer	0.475
Protonic conduction coefficient of membrane	1
Protonic conduction exponent of membrane	1

Table 3
Respective source terms for equations on different regions.

Equation	Flow channel	Gas penetration layer	Catalyst layer	Membrane
Momentum	0	$\frac{\mu}{K_p}\varepsilon^2\vec{u}$	$\frac{\mu}{K_p}\varepsilon_m\varepsilon_{mc}\vec{u} + \frac{K_\phi}{K_p}Z_f C_f F\nabla\phi_e$	$\frac{\mu}{K_p}\varepsilon_m\varepsilon_{mc}\vec{u} + \frac{K_\phi}{K_p}Z_f C_f F\nabla\phi_e$
Energy	0	0	$\frac{\lvert j_c\rvert}{2F}T\lvert\Delta s\rvert + \lvert j_c\eta_c\rvert$(cathode)0(anode)	$\frac{I^2}{\sigma_e}$
Chemical forms	0	0	$\frac{j_a}{2FC_{tot,a}}(H_2)$ $\frac{j_c}{4FC_{tot,c}}(O_2)$ $\frac{j_c}{2FC_{tot,c}}(H_2O)$	0
Solid phase and membrane potential	0	0	j	0

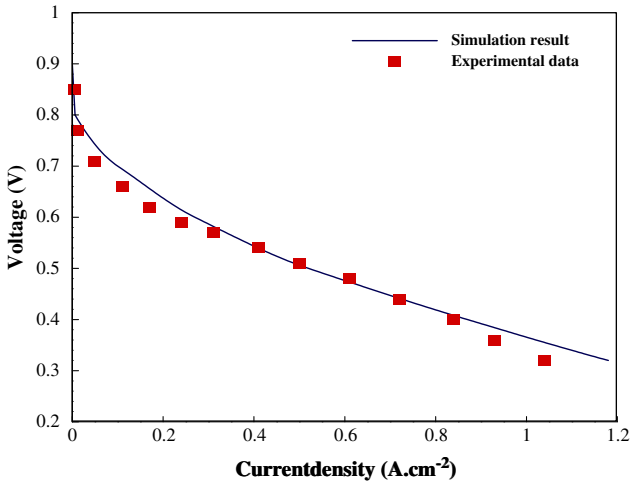

Fig. 5. Polarity curve obtained from numerical approach compared against experimental data.

inlet gases is 100%. Considering the fact that conditions for numerical simulations are analogous to those for experiments a good agreement is observable between the results ensued from each approach.

The difference between experimental and numerical obtained results in low current densities is up to 8% and the maximum difference is related to higher currents and the amount is 10%. There is a problem with reactant gases to react in cathode catalyst in higher current densities because of water flooding and the efficiency of fuel cell decreases intensely. The single phase model has been used and it has no ability to show this complicated phase changing of water in the fuel cell at high current densities. This assumption is logical and convenient in regular flows.

The majority of the research conducted in this area considers air for the inlet flow on the cathode side; however, since only 21% of the air belongs to oxygen, it is expected that if pure oxygen is deployed instead of air, one can observe performance improvement. This trend is detectable in the numerical simulation which utilizes pure oxygen as it is delineated in Fig. 6.

4.2. The effect of inlet gases humidity

Figs. 7 and 8 include numerical and experimental results based upon equal increment in inlet gases humidity on anode and cathode sides for four different humidification strategies.

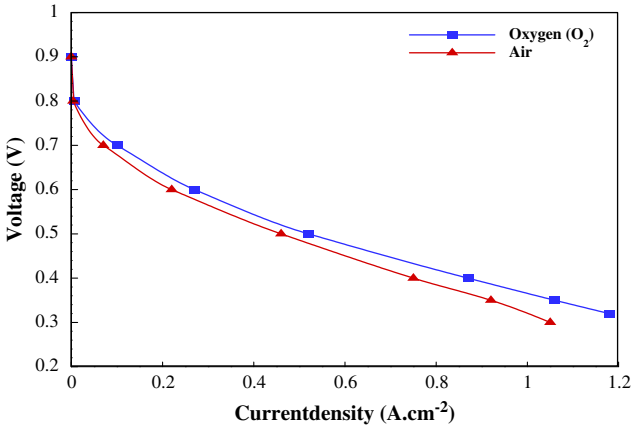

Fig. 6. Effect of employing pure oxygen instead of air on cell performance.

(.i.e. RH = 10–40–70–100%). The results are presented in the form of voltage–current density and also power–current density diagrams. It is observed that performance betterment is detectable with equal humidification for fuel and oxidant on both anode and cathode sides within the range of 10–100% for humidity. The reason could be traced in the idea that changes in water mole fraction duo to increment in relative humidity in inlet gases leads to increase of the water in the membrane which results in reduction in ionic resistance ensuing easier proton transfer leading to increment in the outlet current density at a constant voltage. The obtained results demonstrate the positive impact of humidity increment on power improvement of the fuel cell. It is also observable that in low current densities the effect of humidity alteration is negligible however medial and higher current densities will definitely benefit from such strategy due to considerable drop in Ohmic resistance.

4.3. Hydrogen mass fraction distribution

Fig. 9 includes the results of the simulations depicting hydrogen mass fraction distribution for different values of inlet gases

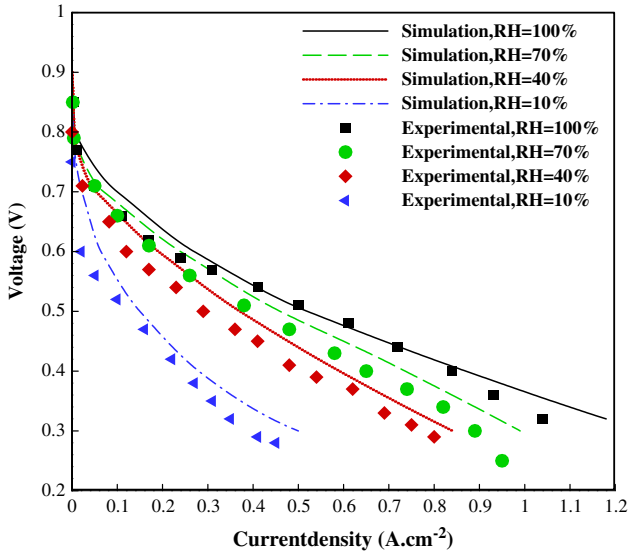

Fig. 7. Effect of inlet gasses temperature on cell performance (*V–I*).

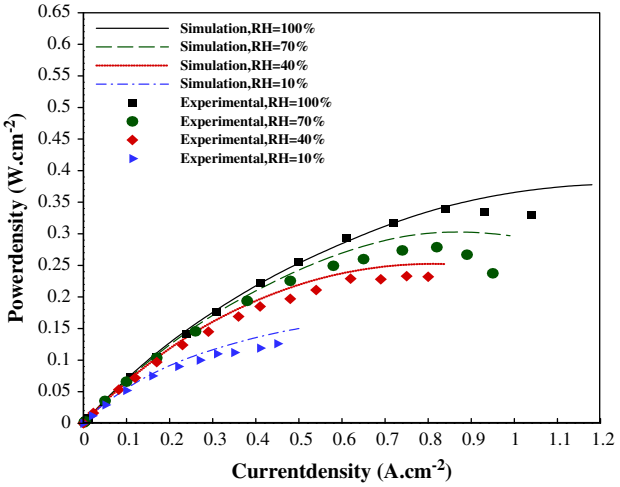

Fig. 8. Effect of inlet gasses temperature on cell performance (*P–I*).

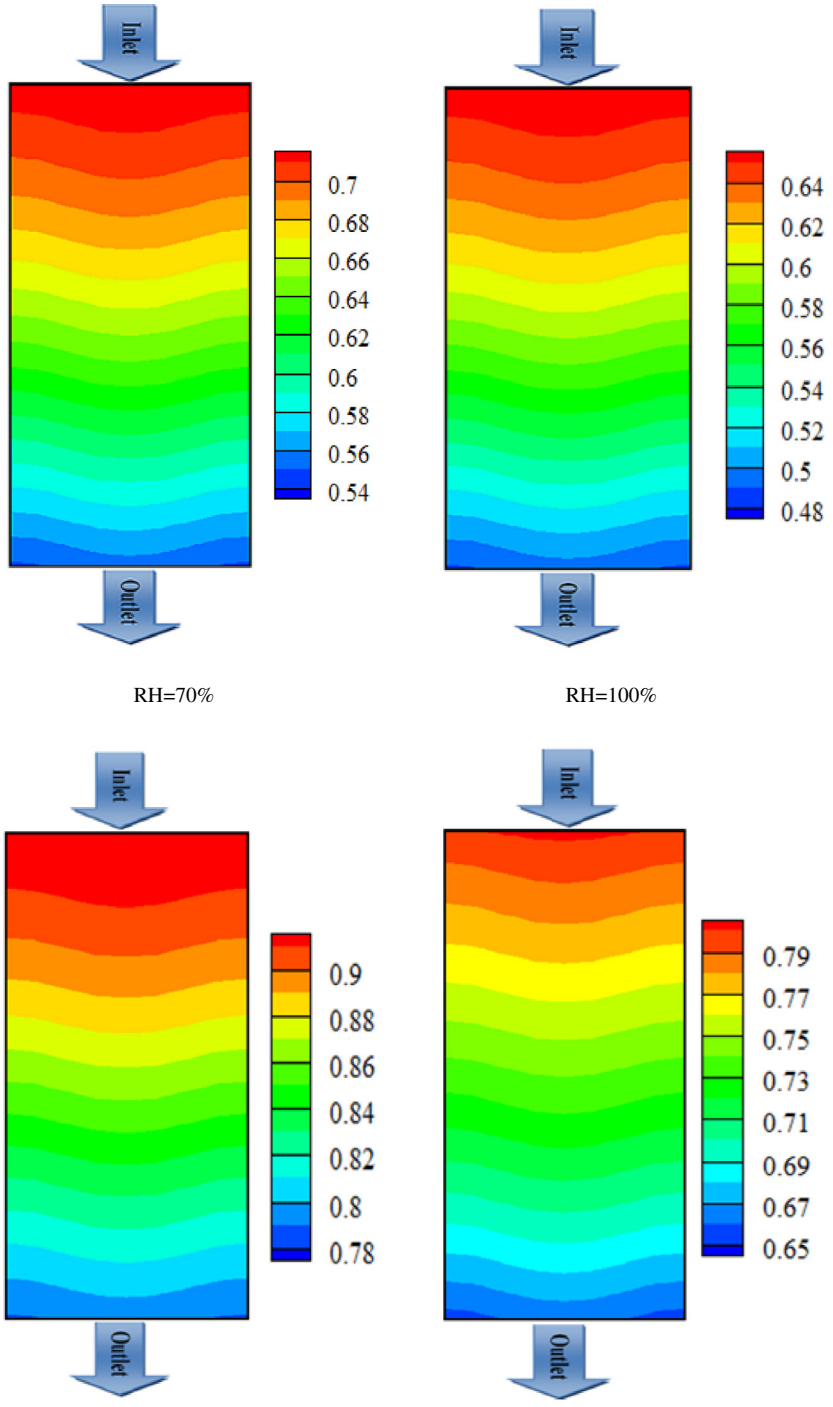

Fig. 9. Hydrogen mass fraction distribution.

humidity in longitudinal direction of the channel, and in the intersection between the membrane and anode side catalyst of the fuel cell. Operating voltage is 0.5 V and the condition presented in Table 4 are applied in these simulations. It is shown that the mass fraction of hydrogen gradually decreases through the channel the reason of which is claimed to be consumption of this gaseous form, it is also observed that this mass fraction experience increment when humidity is reduced, the reason is asserted to be based upon the idea that this alteration leads to decrease in consumption rate of hydrogen.

4.4. Oxygen mass fraction distribution

In Fig. 10 oxygen mass fraction distribution for different values of inlet gases humidity in the intersection between the membrane and cathode side catalyst of the fuel cell are delineated. The results demonstrate that the mass fraction of oxygen decreases through the channel in an inchmeal manner, the reason of this trend is claimed to be consumption of this gaseous form; it is also observed that a similar behavior as hydrogen exists for this mass fraction due to same reasons.

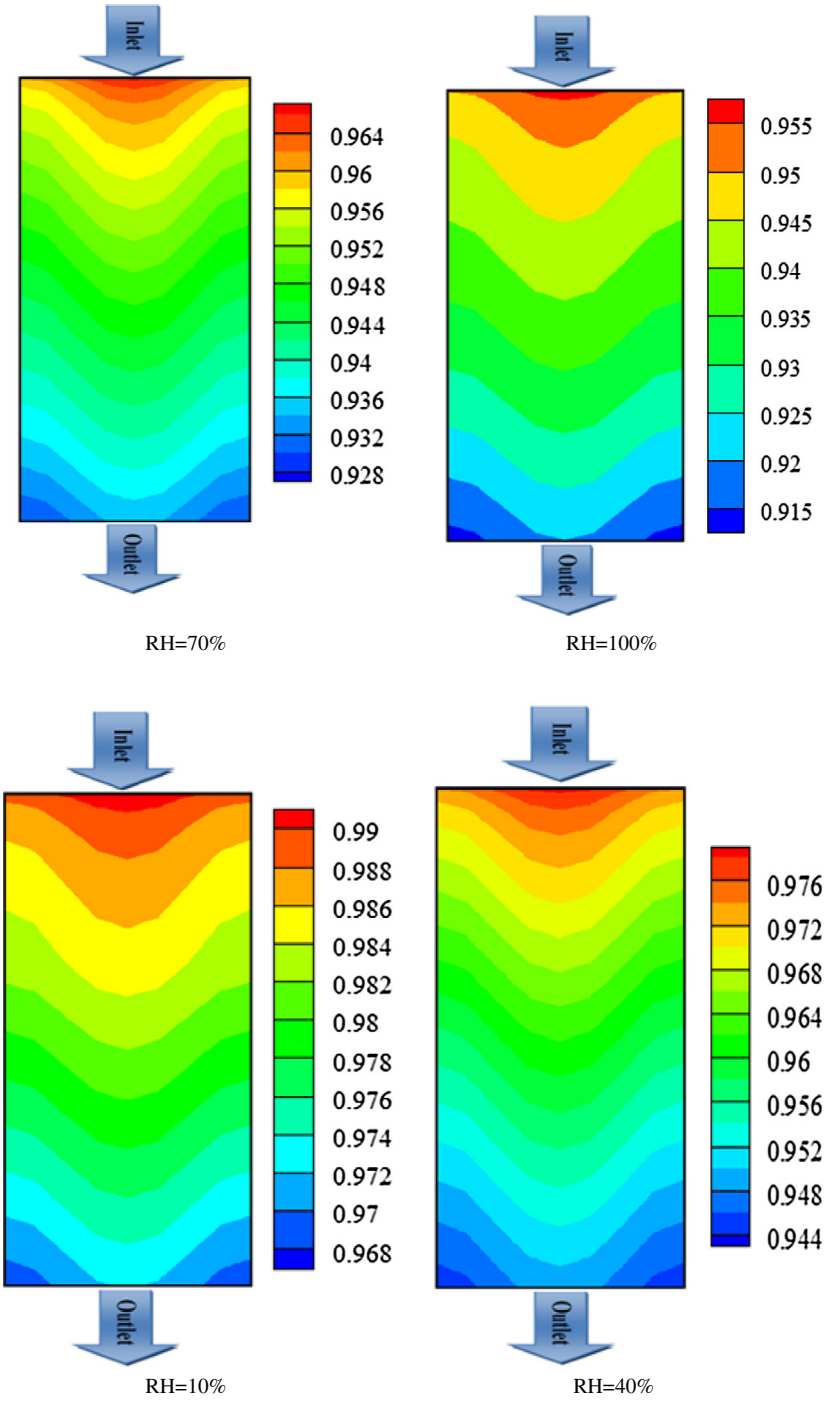

Fig. 10. Oxygen mass fraction distribution.

4.5. Water mass fraction distribution

In a polymer fuel cell water is produced on the cathode side duo to chemical reactions between oxygen and hydrogen. Fig. 11 depicts water mass fraction distribution for different values of inlet gases humidity in the intersection between the membrane and cathode side catalyst of the fuel cell in the direction of fuel cell channel. The results show that mass fraction of water increases through the channel the reason of which is claimed to be consumption of the majority of the gaseous forms. The produced water on the cathode size approaches toward the channel outlet, if this water fail to exit from the cell the porous regions will be blocked which can lead to water leakage to oxygen passage channels. It is also observed that oxygen mass fraction decreases with reduction in humidity, due to the idea that oxygen consumption rate degradation.

I order to achieve a desirable hydration level and consequently minimum Ohmic losses in membrane, fuel and air are introduced to the system in fully humid level in some strategies for fuel cell performance. However, since water is produced on the cathode side, high humidity percentage on the cathode electrode could lead to flooding of cathode gas penetration layer in some cases. This phenomenon will ensue less oxygen availability for electro-chemical process which will cause performance deterioration. In addition, there will be extra investment costs imposed due to inlet

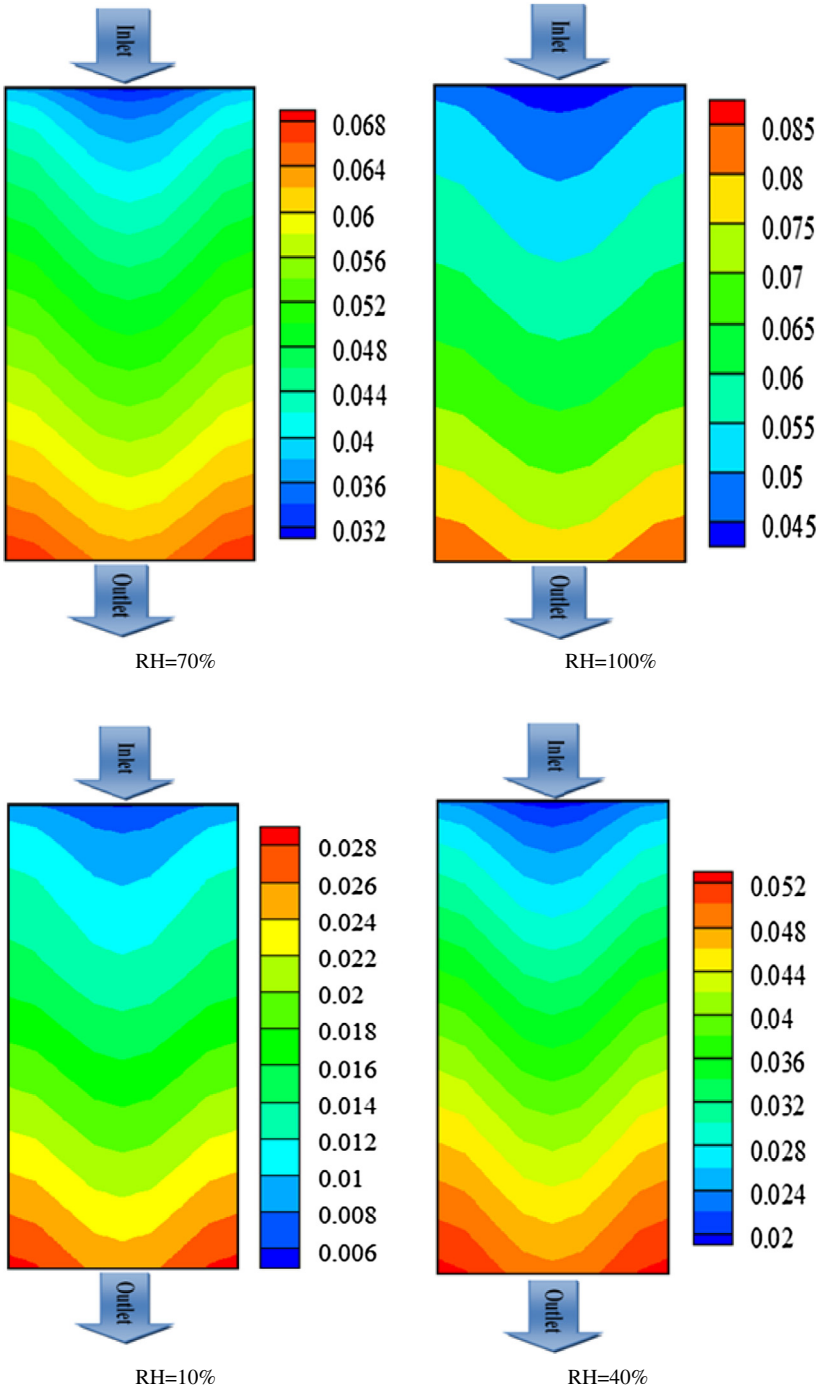

Fig. 11. Water mass fraction distribution.

gases humidification equipment and also some parasitic power will not be avoidable which all make the strategy of lower relative humidity more favorable.

Figs. 12 and 13 include the results of simulation in which the anode side humidity is set at its full state while the cathode side's humidity percentage changes from 10% to 40% and 70%. As can be detected, in comparison with the previously discussed strategy in which the humidity percentage would increase with the same rate for both sides, a considerable amelioration in performance is achieved. Since the possibility of drying on cathode side and flooding on anode side exists, high humidity percentage on the anode side will lead to performance improvement despite lower humidity levels on cathode side.

The results demonstrate that an increment equal to 30% in oxygen humidity (.i.e. from 10% to 40%) will cause increment in current density at a constant voltage; moreover, this increase in relative humidity has led to output power ameliorations. Increasing the humidity from 40% to 70% in high current densities does not benefit the cell performance significantly due to losses in density of the flow.

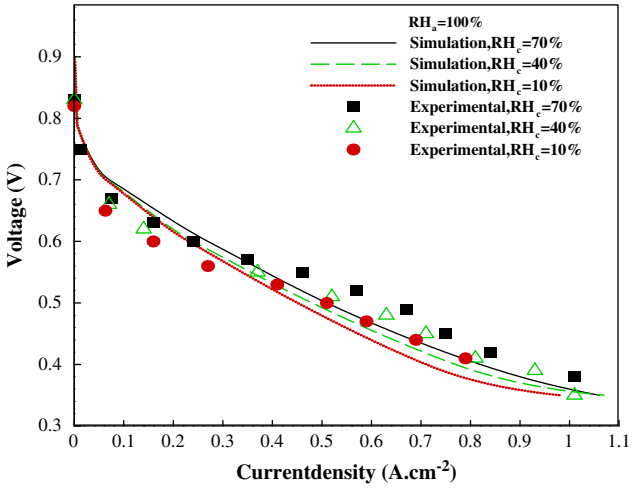

Fig. 12. Effect of oxygen gas humidification on cell performance (*V–I*).

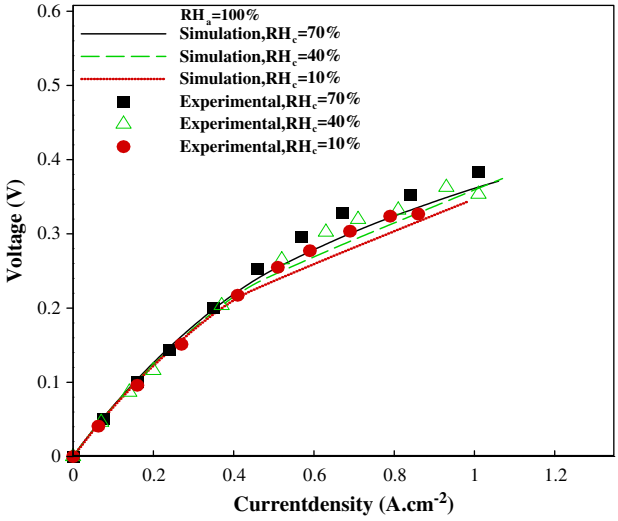

Fig. 13. Effect of oxygen gas humidification on cell performance (*P–I*).

4.6. The effect of inlet mass flow rates

The results obtained through experimental measurements and numerical simulations dealing with the effect of changes in inlet mass flow rates of hydrogen and oxygen on the performance of the fuel cell are shown in Figs. 14–17, and numerical and experimental results are deemed to be at satisfying agreement. Fig. 14 shows voltage–current density diagram while Fig. 15 is dedicated to power–current density diagram, note that the conditions presented in Table 4 apply to these figures and relative humidity for inlet gasses in considered to be 100%, three different mass flow rates for hydrogen gas has been investigated, 0.3, 0.5, and 0.7 l/min. It is observed that when the mass flow rate changes from 0.3 to 0.5 l/min and all the other parameters are maintained constant (i.e. $\dot{m}_{O_2} = 0.5$ l/min), fuel cell performance experiences betterments, while the same alteration in mass flow rate from 0.5 to 0.7 l/min will ensue degradation in voltage and the output power in a constant current density.

According to the obtained results, in the mentions mass flow rates for hydrogen gas, an increment in the mass flow rates, the possibility of penetration throughout the active area increases which leads to fuel cell performance elevation. The results show that when the mass flow rate reaches to 0.7 l/min, the performance

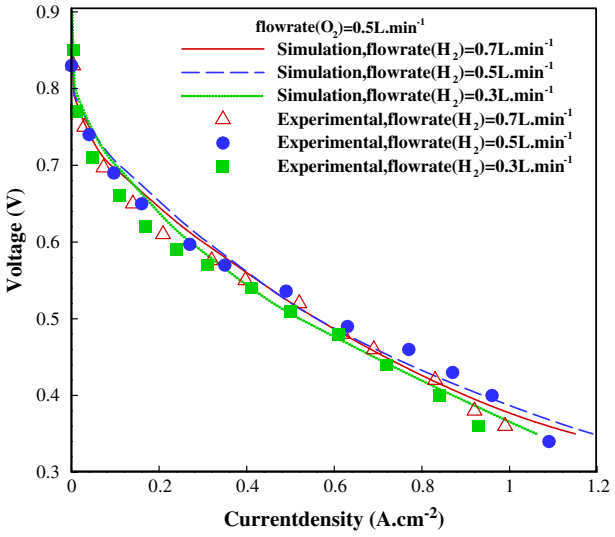

Fig. 14. Effect of hydrogen mass flow rate on cell performance (*V–I*).

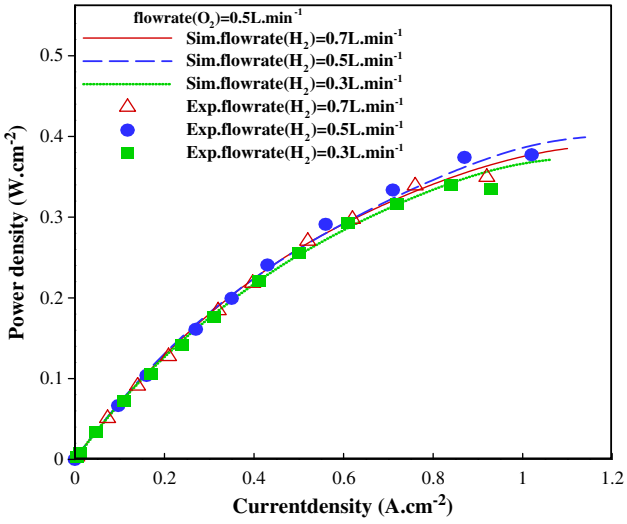

Fig. 15. Effect of hydrogen mass flow rate on cell performance (*P–I*).

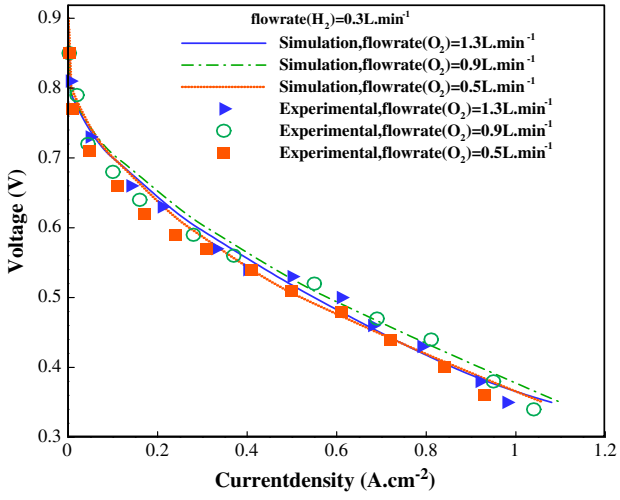

Fig. 16. Effect of oxygen mass flow rate on cell performance (*V–I*).

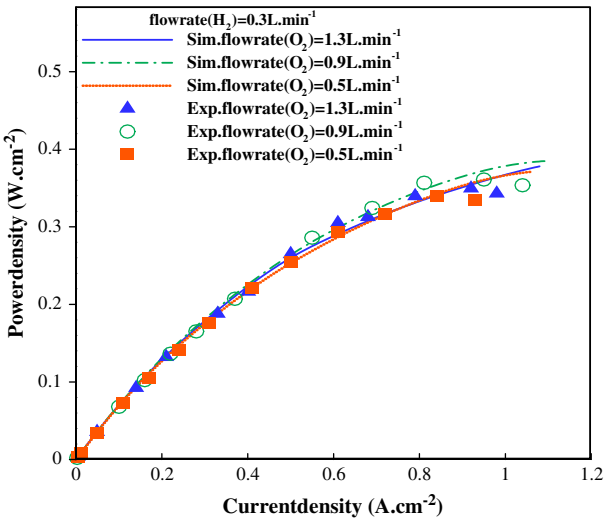

Fig. 17. Effect of oxygen mass flow rate on cell performance (*P–I*).

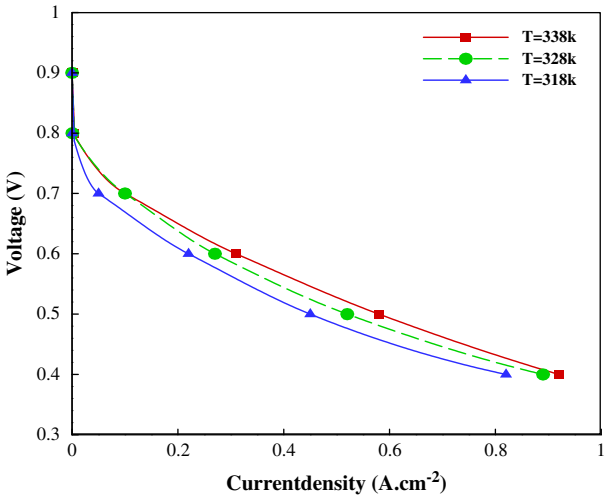

Fig. 18. Effect of inlet gases temperature on cell performance (*V–I*).

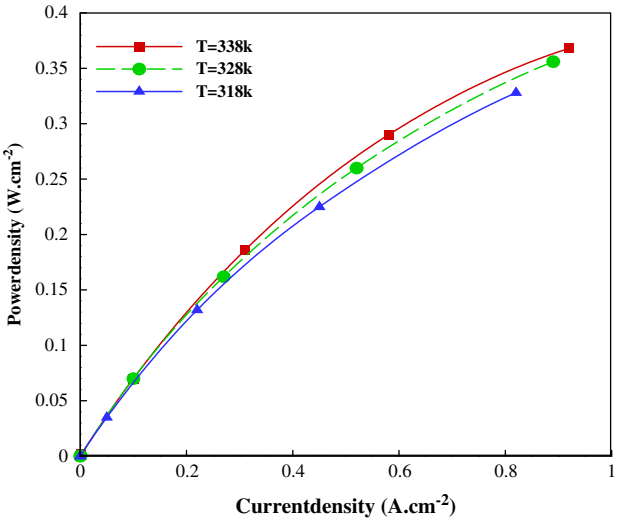

Fig. 19. Effect of inlet gases temperature on cell performance (*P–I*).

deteriorates due to the fact that a considerable amount of employed hydrogen leaves the cell without participating in reaction.

Figs. 16 and 17 show voltage–current density and power–current density diagrams of the conditions presented in Table 4 respectively, three different oxygen mass flow rates (.i.e. 0.5, 0.9, and 1.3 l/min) have been investigated. It is observed that when oxygen inlet mass flow rate changes from 0.5 to 0.9 l/min, with all the others parameters kept constant (i.e. $\dot{m}_{H_2} = 0.3$ l/min), fuel cell performance improves, while the same alteration in mass flow rate from 0.9 to 1.3 l/min will result in reduction in voltage and the output power in a constant current density. Oxygen mass flow rate increments within 0.5–0.9 l/min provide more uniform gas penetration into cathode catalyst area; thus, electro-chemical reactions occur in a more effective manner. The results demonstrate that mass flow rate increments within 0.9–1.3 l/min degrade the performance mostly due to lack of desirable penetration possibility. Moreover, elevation in mass flow rate on the cathode side will drive the water flow toward the exit of the cell which will prevent the flooding phenomenon and help enhancing cell performance; however, this desirable and positive effect applies until a certain point of mass flow rate increment after which drying phenomenon could decrease cell performance.

4.7. The effect of inlet temperature

The effect of inlet gases temperature is delineated in Figs. 18 and 19 considering three different temperature levels. One of the major causes of voltage drop in a fuel cell which leads to reduction of cell's open circuit voltage is the activation loss which occurs in low current densities happening in the beginning of chemical reactions in catalyst layers of the cell. Temperature increments cause enhancement in reaction rates in catalyst layer leading to reduction in activation loss and performance elevation. As can be observed form the mentioned figures, temperature elevation increase the output voltage; actually, when temperature increases ionic conduction coefficient elevates and thusly proton passage within the membrane increases in rate and viability. In weak current densities, there are negligible discrepancies between cell performances due to differences in electro-chemical reaction rates. In medial current densities in which Ohmic losses are dominant in the cell, temperature increase results in ionic conduction elevation and performance enhancement. In high current densities, temperature elevation leads to increase in vapor pressure which prevents performance degradations ensuing from flooding phenomenon. In spite of the fact that in considerably high temperatures temperature increment reduces the effect of transitional losses and elevates electro-chemical rates, this temperature elevation could lead to cell potential degradation due to the possible drying phenomenon. Drying results in ionic conductivity and also thermal stresses are increased in such a case which can result in membrane dismantlement; thus, in this study lower temperature levels are considered for investigation.

4.8. Activation voltage loss distribution

As discussed earlier, in order to start a fuel cell certain amount of energy is required, providing of which results in a voltage drop called "activation voltage loss". Fig. 20 depicts activation voltage loss distribution on the cathode catalyst face for $V = 0.5$ and $V = 0.3$ respectively; note that the conditions provided table to are applied in the investigations.

Considering the absolute value for voltage drop, this value increases with approaching toward the outrance of the face, mostly due to reduction in the density of reacting gases. Beneath the

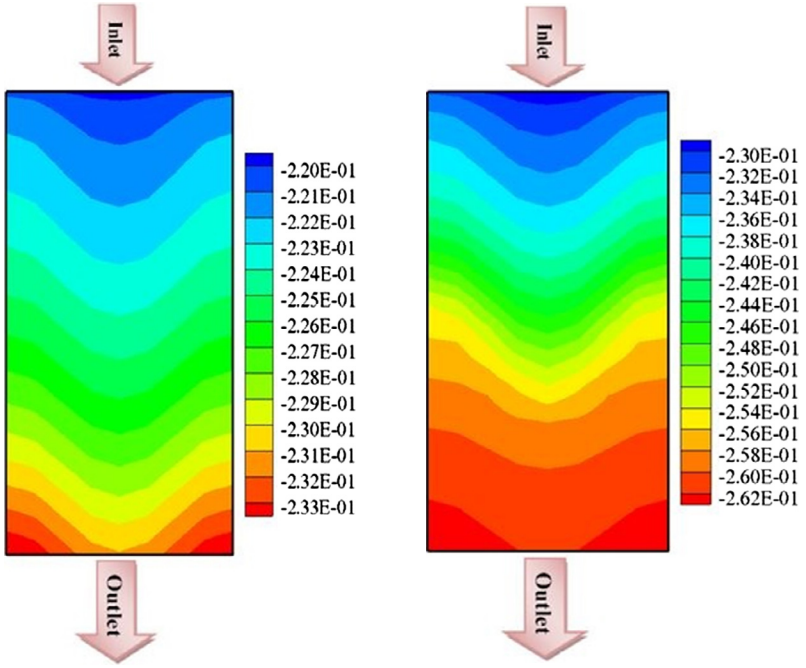

Fig. 20. Activation voltage loss distribution on cathode catalyst face.

polarized face the drops are detected to be more severe in comparison with the above regions of oxygen passage channel. Considering the pattern of loss distribution in the current density, it is observable that these losses are minor in low current densities when compared against higher current density, the reason could be traced in the idea that in higher current densities oxygen consumption rate elevates due to enhancement in reaction rate which leads to reduction in oxygen density resulting in increment in activation voltage loss.

5. Concluding remarks

In this study, a 3D numerical simulation on a polymer membrane fuel cell is conducted in various working conditions including different relative humidity with constant humidity percentages on the anode and cathode sides; moreover, humidity percentage equal to 100% on the anode side with different humilities on the cathode sides, and inlet gases temperature elevation are investigated, the following includes the obtained remarks from this study:

1. Employing pure oxygen instead of air in fuel cell leads to elevation in current density in a constant voltage on the polarity curve and results in cell performance enhancement, mostly due to the fact that air includes merely 21% oxygen which participates in the electro-chemical reaction.
2. Equal increment in inlet gases humidity on both anode and cathode sides from 10% to 100% for four different humidity percentage of 10%, 40%, 70%, and 100% leads to reduction in ionic resistance in the membrane and consequently performance improvement.
3. Mass fraction of hydrogen and oxygen gasses decreases gradually throughout the channel, which occurs mainly due to consumption of these gaseous forms. With degradation in humidity these consumption rates decrease and it is observed that oxygen mass fraction elevates.
4. The amount of produced water increases throughout the channel due to water production and it's accumulation in the cathode exit path.
5. When humidifying the inlet gases from 10% to 70% on the cathode side considering a fully humid anode side (RH_a = 100%), the best fuel cell performance is detected when cathode's humidity is deemed equal to 70%. It shows when the percent of humidity at anode side is high, even with poor humidity at cathode side, the efficiency is higher than the situation that both sides have the same percent of humidity. Anode side needs more humidity for preventing the membrane from drought and the cathode side needs less humidity because of producing water and avoiding from flooding.
6. Increment in inlet hydrogen mass flow rate from 0.3 to 0.5 l/min while the inlet oxygen mass flow rate is kept constant at 0.5 l/min, improves the fuel cell performance. When hydrogen mass flow rate is increased further to 0.7 l/min, cell performance experiences degradation due to the fact that a considerable amount of inlet hydrogen leaves the cell without participating in chemical reaction.
7. Elevation in inlet oxygen mass flow rate from 0.7 to 0.9 l/min while the inlet hydrogen mass flow rate is maintained at 0.3 l/min, amelioration in fuel cell performance is observable. While further increments in oxygen mass flow rate from 0.9 to 1.3 degrades the performance.
8. Temperature elevation in three cases of 318, 328, and 338 K enhances the performance of the cell on the polarity curve and on power density versus current density diagram, due to improvements in membrane protonic conductivity.
9. When approaching the outrance of the cathode catalyst face, activation voltage loss increases due to reductions in reactor gases density. Activation voltage losses are minor in low current densities in comparison against higher current densities. In higher current densities oxygen consumption rate elevates due to increase in reaction rate which leads to reduction in oxygen density resulting in severe activation voltage losses.

References

[1] Jhanwar JC, Jethwa JL. The use of fuel cells in production blasting in an open pit coal mine. Geotechn Geolog Eng J 2000;18:269–87.

[2] Afshari E, Jazayeri SA. Water management in a PEM fuel cell using two phase single-domain model. In: Proceedings of ASME, European Fuel Cell Technology & Applications, Rome, Italy, December 11–14, 2007.

[3] Pasaogullari U, Wang CY. Two-phase modeling and flooding prediction of polymer electrolyte fuel cells. J Electrochem 2005;152:A380–90.

[4] Iranzo A, Boillat BP, Biesdorf BJ, Salva A. Investigation of the liquid water distributions in a 50 cm^2 PEM fuel cell: effects of reactants relative humidity, current density, and cathode stoichiometry. J Energy 2015;82:914–21.

[5] Mulyazmi, Daud WRW, Majlan EH, Rosli MI. Water balance for the design of a PEM fuel cell system. J Hydrogen Energy 2013;38:9409–20.

[6] Al-Zeyoudi H, Sasmito AP, Shamim T. Performance evaluation of an open-cathode PEM fuel cell stack under ambient conditions: case study of United Arab Emirates. Energy Convers Manage 2015;105:798–809.

[7] Bozorgnezhad A, Shams M, Kanani H, Hasheminasab M, Ahmadi G. The experimental study of water management in the cathode channel of single-serpentine transparent proton exchange membrane fuel cell by direct visualization. Int J Hydrogen Energy 2015;40:2808–32.

[8] Reshetenkoa TV, Benderb G, Bethunea K, Rocheleaua R. Systematic studies of the gas humidification effects on spatial PEMFC performance distributions. J Electrochim Acta 2012;69:220–9.

[9] Sreenivasulu B, Vasu G, Dharma Rao V, Naidu SV. Performance study of a PEM fuel cell with 4-Serpentine flow fields-experimental study. J Eng Sci Adv Technol 2012;2:291–6.

[10] Sreenivasulu B, Naidu SV, Rao V Dharma, Vasu G. A theoretical simulation of a PEM fuel cell with 4-Serpentine flow channel. Int J Comput Eng Res 2012;2:97–106.

[11] Wong K, Loo K, Lai Y, Tan S-C, Chi KT. A theoretical study of inlet relative humidity control in PEM fuel cell. Int J Hydrogen Energy 2011;36(18):11871–85.

[12] Yuan W, Tang Y, Li z, Pan M, Li Z, Tang B. Model prediction of effects of operating parameters on proton exchange membrane fuel cell performance. J Renewable Energy 2010;35:656–66.

[13] Jeon Dong Hyup, Kim Kwang Nam, Baek Seung Man, Nam Jin Hyun. The effect of relative humidity of the cathode on the performance and the uniformity of PEM fuel cells. Int J Hydrogen Energy 2011;36(19):12499–511.

[14] Rosli MI, Borman DJ, Ingham DB, Ismail MS, Ma L, Pourkashanian M. Transparent PEM fuel cells for direct visualization experiments. Fuel Cell Sci Technol 2010;7(6):61015–21.

[15] Afshari E, Jazayeri SA. Performance analysis of a polymer electrolyte fuel cell system for automotive application. J Engine Res 2009;16(Autumn).

[16] Um S, Wang CY, Chen KS. Computational fluid dynamics modeling of proton exchange membrane fuel cells. J Electrochem Soc 2000;147(12):4485–93.

[17] Springer TE, Zawodzinski TA, Gottesfeld S. Polymer electrolyte fuel cell model. J Electrochem 1991;136:2334–42.

[18] Springer T, Zawodzinski T, Gottesfeld S. Electrode materials and process for energy conversion and storage. J Electrochem Soc 1997;13:1–14.

[19] Chua HS, Wang a CP, Liao a WC, Yan WM. Transient behavior of CO poisoning of the anode catalyst layer of a PEM fuel cell. J Power Sour 2006;160:340–52.